

Be-star rotation: how close to critical?

R. H. D. Townsend,^{1,2*} S. P. Owocki^{1,2} and I. D. Howarth¹

¹*Department of Physics & Astronomy, University College London, Gower Street, London WC1E 6BT*

²*Bartol Research Institute, University of Delaware, Newark, DE 19716, USA*

Accepted 2004 January 15. Received 2004 January 14; in original form 2003 July 29

ABSTRACT

We argue that, in general, observational studies of Be-star rotation have paid insufficient attention to the effects of equatorial gravity darkening. We present new line-profile calculations that emphasize the insensitivity of line width to rotation for fast rotators. Coupled with a critical review of observational procedures, these calculations suggest that the observational parameter $v \sin i$ may systematically underestimate the true projected equatorial rotation velocity, $v_e \sin i$, by some tens of per cent for rapid rotators. A crucial implication of this work is that Be stars may be rotating much closer to their critical velocities than is generally supposed, bringing a range of new processes into contention for the elusive physical mechanism responsible for the circumstellar disc thought to be central to the Be phenomenon.

Key words: line: profiles – techniques: spectroscopic – stars: emission-line, Be – stars: fundamental parameters – stars: rotation.

1 INTRODUCTION

Be stars are near-main-sequence, B-type stars that have been observed to show Balmer-line emission. It is approaching a century and a half since the discovery of the first Be star (Secchi 1867), and in recent decades compelling empirical evidence has associated the emission-line episodes with the formation of quasi-Keplerian, equatorial discs (e.g. Dachs et al. 1986; Hanuschik 1996). However, there is still no general agreement on the underlying physical mechanisms responsible for disc formation (cf. Smith, Henrichs & Fabregat 2000).

A phenomenologically crucial characteristic of Be stars is that they rotate rapidly – more rapidly than any other class of non-degenerate star. Virtually as soon as this was recognized, it was hypothesized that the equatorial rotation velocities, v_e , may be sufficiently close to the critical velocity, v_c , for material easily to ‘leak’ into a disc (Struve 1931; here v_c is the velocity at which centrifugal forces balance Newtonian gravity at the equator, so that the effective gravity, g_{eff} , vanishes). Slettebak and others later scrutinized this hypothesis quantitatively (e.g. Slettebak 1949, 1966; Slettebak, Collins & Truax 1992), establishing the current canonical view that the rotation of Be stars is actually significantly *subcritical*, with $v_e/v_c \simeq 0.7$ – 0.8 (e.g. Porter 1996; Chauville et al. 2001).

If rotation does play a direct, causal role in the Be phenomenon, then it is tempting to speculate that it does so by reducing the effective equatorial gravity to an extent that allows ‘weak’ processes to move material into orbit easily (Owocki 2002). However, if this is to be a promising avenue of exploration, then rotation must be much closer to the critical value than is generally supposed at present:

at $v_e/v_c \simeq 0.7$ the equatorial gravity is reduced by only about a factor of 2, and it requires $v_e/v_c \simeq 0.95$ to reduce g_{eff} by an order of magnitude. Alternatively, to launch material into orbit ballistically at $v_e/v_c = 0.7$ requires velocities in excess of 100 km s^{-1} ; launch velocities commensurate with the speed of sound (at which the aforementioned weak processes typically operate) are achieved only when a rotation rate $v_e/v_c \simeq 0.95$ is reached. Similar arguments may be brought to bear on the angular-momentum budget needed to achieve orbit.

In the present paper we review the bases for determining the true projected equatorial rotation velocity, $v_e \sin i$, and the relationship to its observational counterpart $v \sin i$ (where i is the angle between the line of sight and the rotation axis). We argue that equatorial gravity darkening may plausibly have led to rotational velocities of Be stars being systematically underestimated, and that Struve’s original hypothesis of near-critical rotation in Be stars therefore has not been ruled out by existing observational studies.

2 PREAMBLE

For a centrally condensed star, the critical velocity of rotation is given by

$$v_c = \sqrt{GM_*/R_e} = \sqrt{2GM_*/3R_p}, \quad (1)$$

where the ‘e’ and ‘p’ subscripts are used throughout to denote equatorial and polar values, respectively (we assume uniform angular velocity at the stellar surface). We note that, even if it were possible to measure the equatorial rotation velocity with complete accuracy, these expressions imply considerable observational uncertainty in establishing v_c . In particular, it is customary to adopt masses and radii from look-up tables, on the basis of spectral type; and yet not

*E-mail: rhdt@bartol.udel.edu

only is the spectral type affected by rotation, in an aspect-dependent manner (e.g. Slettebak, Kuzma & Collins 1980), but the physical relationship between spectral type, mass and radius is also modified (Maeder & Meynet 2000). Thus systematic errors in v_e/v_c may easily arise from this source alone.

The primary focus here, however, is on the determination of $v_e \sin i$. Almost all published surveys of rotational velocities in Be stars rely on one of two approaches. The first is to infer $v_e \sin i$ values from, typically, line width at half depth, calibrating the results through the standard-star system established by Slettebak et al. (1975) or its extension to rapid rotators (Slettebak 1982). The second is to compare observations with ‘spun-up’ versions of narrow-line stars¹ or model-atmosphere flux spectra, typically using a convolution approach (cf. Gray 1992). We emphasize that the latter approach is unphysical: the convolution between intrinsic line profile and Doppler broadening function assumes the two to be independent, which is clearly not the case when the stellar surface parameters (i.e. T_{eff} and g_{eff}) vary with latitude.

Both techniques imply the assumption of a single-valued, (approximately) linear relationship between the line width and $v_e \sin i$. As we demonstrate below, the true situation is significantly more complicated. In particular, for a rigidly rotating star with radiative envelope that follows the von Zeipel (1924) form for gravity darkening,

$$T_{\text{eff}} \propto g_{\text{eff}}^{0.25}, \quad (2)$$

the contribution of the cooler (and hence fainter) equatorial regions to the observed spectrum may be reduced to the point where they are effectively invisible. A necessary consequence of such behaviour is that $v \sin i$ values determined without proper attention to gravity darkening will systematically underestimate true projected equatorial velocities. This point is developed in the following sections, through the use of illustrative calculations and by a critical review of observational studies.

3 MODELS

In Table 1 we introduce parameters for 13 stellar models, representative of the spectral types² spanning the B0–B9 interval. The mass and polar radius of the models in Table 1 are taken from Porter (1996), with the critical velocity evaluated using equation (1). To obtain the accompanying luminosity data we use the Warsaw–New Jersey code³ to calculate evolutionary tracks at the masses tabulated by Porter, determining L_* from the epoch at which the radius coincides with Porter’s values.

For each of the 13 stellar models, we construct two sequences, differing only in the treatment of the centrifugal force owing to rotation. For the ‘complete’ set of models, the effects of this force are fully

¹ Not necessarily corresponding to slowly rotating stars.

² We stress that here, and throughout, our use of the term ‘spectral type’ in reference to our models is little more than a notational convenience: although, for instance, a non-rotating star with the same parameters as our B0 model will exhibit a spectrum loosely resembling a star with MK type B0, it should always be remembered that the MK scheme (e.g. Morgan & Keenan 1973) is *two-dimensional*, and variations in a third parameter, such as rotation, negate any direct correspondence with specific physical parameters.

³ Details of this code are given in Dziembowski, Moskalik & Pamyatnykh (1993) and Dziembowski & Pamyatnykh (1993), the only significant difference in the present work being the adoption of more recent OPAL tabulations for opacity (Iglesias & Rogers 1996) and equation of state (Rogers, Swenson & Iglesias 1996).

Table 1. Fundamental parameters for the B-type models considered herein.

Sp. Subtype	M_* (M_\odot)	R_p (R_\odot)	v_c (km s^{-1})	$\log L_*$ (dex L_\odot)
B0	17.5	7.7	538	4.64
B0.5	14.6	6.9	519	4.41
B1	12.5	6.3	502	4.21
B1.5	10.8	5.7	491	4.01
B2	9.6	5.4	475	3.85
B2.5	8.6	5.0	468	3.68
B3	7.7	4.7	456	3.52
B4	6.4	4.2	440	3.24
B5	5.5	3.8	429	3.00
B6	4.8	3.5	418	2.78
B7	4.2	3.2	408	2.56
B8	3.8	3.0	401	2.39
B9	3.4	2.8	393	2.20

accounted for: the surface geometry is that of a gravitational equipotential within the Roche approximation, and the surface temperature distribution follows the von Zeipel (1924) gravity-darkening law appropriate to radiative envelopes (cf. equation 2). The luminosity L_* is preserved under changing model geometry by adjusting the polar effective temperature in accordance with the relationship

$$T_p = \left(\frac{g_p L_*}{\sigma \Sigma_1} \right)^{0.25}; \quad (3)$$

here, σ is the Stefan–Boltzmann constant, and Σ_1 is the surface-area-weighted gravity of the rotating star (e.g. Cramer 1996).

By contrast, for the ‘uniform’ set of models the centrifugal force is neglected, so that the star remains spherical in shape, and exhibits a uniform surface temperature and gravity; these models mimic the traditional methodology developed by Carroll (1928) and Shajn & Struve (1929), which is the basis for the convolution approach described by Gray (1992) and used by many authors (e.g. Howarth et al. 1997; Chauville et al. 2001).

4 SPECTROSCOPIC SIMULATIONS

4.1 Method

For both sets of surface models, we synthesize profiles for He I $\lambda 4471$ and Mg II $\lambda 4481$ (including doublet and forbidden components), the lines most commonly used by observers to determine B-star $v \sin i$ values. The calculations use the BRUCE code (Townsend 1997), which is readily adapted from its original intended application in modelling non-radial pulsation by simply setting the pulsation amplitudes to zero.

A large grid of precomputed conventional model spectra is required by BRUCE to describe the angular and wavelength dependences of the photospheric radiative intensity over the range of T_{eff} , $\log g$ values encountered between pole and equator. We construct such a grid using the SYNSPEC spectral-synthesis code by I. Hubeny and T. Lanz. For the B0–B5 models, the underlying atmospheric structure is calculated using the non-LTE TLUSTY code (Hubeny 1988; Hubeny & Lanz 1995), under the assumption that hydrogen and helium are the only sources of line opacity; for the later subtypes, atmospheric models are taken from the line-blanketed LTE grids published by Kurucz (1993).

The rotating-star spectral synthesis is undertaken over a range of equatorial velocities $0 < v_e < v_c$, and at four differing inclinations:

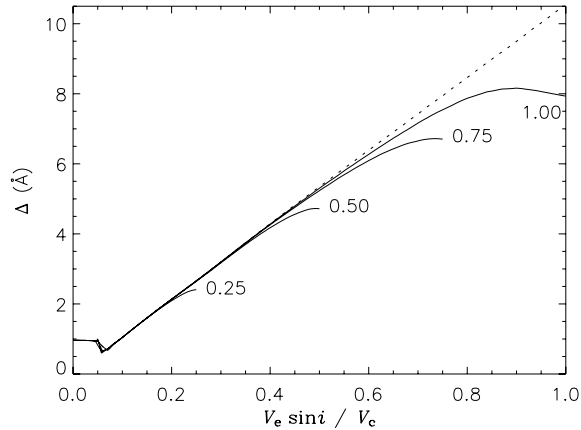


Figure 1. The characteristic widths, Δ , of the He I $\lambda 4471$ line profile for the B2 subtype, plotted as a function of $v_e \sin i$ for the two models and four separate inclinations considered in the text. The width data of the complete model (solid lines) are labelled with their associated $\sin i$ values; those of the uniform model (dotted line) all lie on the same curve. For $v_e \sin i \lesssim 0.05 v_c$, the intrinsic line broadening and blended components dominate rotational effects, and the characteristic widths should be disregarded.

$\sin i = \{0.25, 0.50, 0.75, 1.00\}$. We characterize the line widths of the resulting profiles using the first zero, ξ_1 , of the Fourier transform of the flux spectrum (Smith & Gray 1976); specifically, we use $\Delta \equiv \xi_1^{-1}$. These characteristic widths Δ have a nearly linear relationship with full-width at half depth, but in any case our results are largely insensitive to the particular approach used to characterize line width.

To examine the robustness of our calculations, we computed a number of variants on the basic models, including different choices of stellar parameters (e.g. those published by Slettebak et al. 1992), and alternative parameterizations of the effects of rotation (e.g. fixing the polar temperature, rather than varying it in accordance with equation 3). These variants introduce only small quantitative changes in the results.

4.2 Results: B2 subtype

We first consider the surface models for the B2 subtype, the most common in the sample of known Be stars (see, e.g. Porter 1996). Fig. 1 shows the characteristic widths of the He I $\lambda 4471$ line as a function of $v_e \sin i$, at each of the four $\sin i$ values considered herein, for both the uniform (Δ_u) and the complete (Δ_c) models. We note that the four solid lines each span a different $v_e \sin i$ range because the domain $v_e = [0, v_c]$ has been scaled by the four different $\sin i$ values; a similar effect is not apparent in the dotted lines, because the Δ_u curves of the uniform models are self-similar,⁴ and lie atop one another. The latter result is a corollary of the fact that line widths for the uniform model follow a linear relationship with $v_e \sin i$.

Unlike the uniform models, the characteristic width curves for the gravity-darkened ‘complete’ models (which furnish a better representation of real stars) are *not* self-similar, an embodiment of departures from a linear $\Delta_c - v_e \sin i$ relationship. Such departures arise from a number of effects, including the variations of both line and continuum strength with latitude, but the dominant factor for fast rotators is the decrease in continuum emission near the equator resulting from von Zeipel darkening. This leads to a relatively small contribution from the fast-rotating equatorial regions to the spa-

⁴ By this, we mean that one curve can be transformed into another by scaling both Δ_u and $v_e \sin i$ by the same amount

tially integrated spectrum, and in turn to a systematic reduction in line widths relative to the uniform model. Thus if $v \sin i$ values are calculated using the calibration found for the uniform model, they may underestimate the true value of $v_e \sin i$ by ~ 20 per cent, or more. Moreover, the near-invisibility of the equatorial regions in near-critical rotators means that *increasing v_e has almost no effect on line width* for such stars.

We illustrate this line width redundancy in Fig. 2, for models with $v_e = 395$ and 460 km s^{-1} (0.83 and $0.97 v_c$, respectively). Clearly, even with our effectively noise-free synthetic data, the helium profiles are almost indistinguishable in terms of their widths; there is no practicable means of ascertaining that the two profiles shown belong to models with equatorial velocities that differ by almost 20 per cent. This underlines the point that the degeneracy of Δ_c as a function of v_e must seriously compromise any attempt at devising a $v \sin i(\Delta)$ calibration, and particularly a single-valued, near-linear calibration, for stars strongly affected by gravity darkening.

Also shown in Fig. 2 are the Mg II $\lambda 4481$ profile for the same $v_e = 395$ and 460 km s^{-1} models. The equivalent width (EW) of this line increases with decreasing temperature (by a factor of 2 from pole to equator in our $v_e = 0.95 v_c$ models), unlike the He I lines. This increase in relative line strength partly offsets the decline in continuum flux (which falls by a factor of nearly 4, from pole to equator), and as a result the Mg line widths show a somewhat greater (though still small) response to increasing equatorial rotation.

4.3 Results: other subtypes

The surface models for the other subtypes exhibit behaviour similar to the B2 models discussed above: with the onset of significant gravity darkening, the widths of line profiles saturate, and become insensitive to any further increase in the equatorial velocity. To quantify succinctly the degree of this effect, we measure the line width for complete models at $\sin i = 1$, $v_e/v_c = 0.95$, and then use the uniform models to infer a $v \sin i$ value for that width. We denote the difference ($v_e \sin i - v \sin i$) as a ‘velocity deficiency’, δV , which we list in Table 2 for each of the 13 subtypes considered.

In both the He I and Mg II lines, there is a systematic increase in the velocity deficiency (expressed as a fraction of v_c) toward later spectral types. For the most part, this increase arises from an enhancement of the continuum gravity-darkening effect, as measured by the ratio between polar and equatorial continuum fluxes: in the $\lambda\lambda 4471\text{--}4481$, region appropriate to the He I and Mg II lines, this ratio is 3.7 for the B0 models, but grows to 7.0 for the B9 models. We note in passing that when *bolometric* fluxes are considered, the flux ratio is fixed at ≈ 14.7 by dint of the fact that $v_e/v_c = 0.95$, irrespective of which model is under consideration.

The overall increase in $\delta V/v_c$ toward later spectral types is modulated by the dependence of line EW on temperature. As discussed in the preceding section, the EW variation of the Mg II line tends to counteract the continuum gravity-darkening effect. This explains why the velocity deficiencies exhibited by the line are smaller than those of the He I line, and also why the growth in $\delta V/v_c$ is seen to reverse itself temporarily around subtype B5.

5 PHOTOMETRIC SIMULATIONS

5.1 Method

In the preceding section, we have demonstrated how gravity darkening can make a near-critical star appear, when observed spectroscopically, to be rotating at an ostensibly slower rate. In this section, we broaden our investigation by examining the impact of

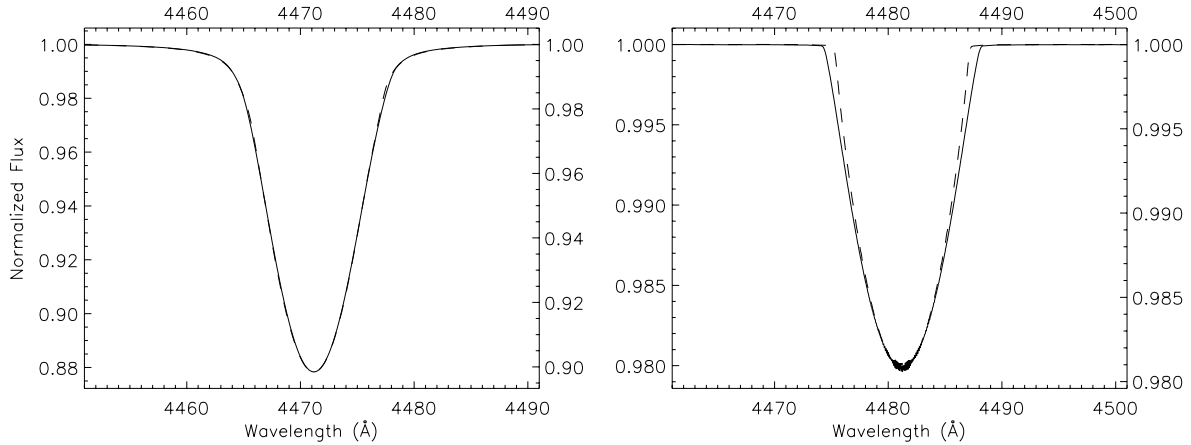


Figure 2. He I $\lambda 4471$ and Mg II $\lambda 4481$ line profiles for equator-on ‘complete’ B2 models at $v_e = 395 \text{ km s}^{-1}$ (solid lines, left-hand scales) and $v_e = 460 \text{ km s}^{-1}$ (dashed lines, right-hand scales). To facilitate the comparison of line widths and shapes, the models are plotted on slightly different vertical scales, chosen so as to normalize the line depths.

Table 2. Velocity deficiencies δV , as a percentage of the critical velocity v_c , for the He I $\lambda 4471$ and Mg II $\lambda 4481$ profiles of the 13 model subtypes; in each case, $v_e/v_c = 0.95$ and $i = 90^\circ$.

Sp. Subtype	$\delta V/v_c$ (per cent)	
	He I $\lambda 4471$ Å	Mg II $\lambda 4481$ Å
B0	12.1	8.7
B0.5	13.7	10.0
B1	15.4	11.0
B1.5	17.0	11.0
B2	18.5	11.4
B2.5	20.0	11.5
B3	21.6	11.9
B4	24.3	12.8
B5	24.6	12.0
B6	26.6	12.5
B7	28.9	14.0
B8	30.8	15.4
B9	33.4	17.1

gravity darkening on the *photometric* signatures of rapidly rotating stars.

For the complete surface models (cf. Section 3), we synthesize absolute magnitudes in the Johnson B and V bands. The calculations use our ROTCOLOR code, which is based on the BRUCE code but oriented toward photometric rather than spectroscopic modelling. ROTCOLOR requires an input grid of precomputed photometric fluxes, which we obtain by combining the four-coefficient limb-darkening data published by Claret (2000) with normal-emergent absolute flux data made available to us by Claret (personal communication); both data are based on the Kurucz (1993) atmosphere grids. To convert synthetic fluxes into absolute magnitudes, we use the observed values for the Sun, $M_B = 5.48$ and $M_V = 4.83$ (Allen 1976).

Our calculations are undertaken for five rotation velocities, $v_e/v_c = \{0.00, 0.24, 0.48, 0.71, 0.95\}$, and at three differing inclinations $i = \{0^\circ, 45^\circ, 90^\circ\}$. For comparison purposes, we also synthesize colours for the evolutionary tracks calculated in Section 3; each track extends from zero-age main sequence (ZAMS) through to terminal-age main sequence (TAMS, defined by the cessation of core hydrogen burning).

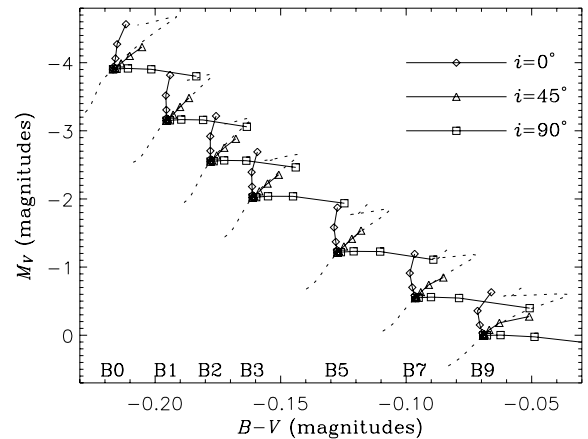


Figure 3. Selected complete surface models (cf. Section 3) plotted as points in the Johnson $B - V$ colour–magnitude diagram, at five rotation velocities $v_e/v_c = \{0.00, 0.24, 0.48, 0.71, 0.95\}$ and three inclinations $i = \{0^\circ, 45^\circ, 90^\circ\}$. Solid lines join together the points from models that differ solely in their rotation velocity; dotted lines indicate ZAMS–TAMS evolutionary tracks that pass through the non-rotating models, the latter being labelled at the bottom of the plot with their nominal spectral types.

5.2 Results

In Fig. 3 we plot the results of our photometric simulations in a colour–magnitude diagram. The general effect of rotation is to displace models away from their zero-rotation loci, moving them along trajectories in the $M_V/(B - V)$ plane that are, to a first approximation, straight lines. The differential rate of displacement varies in step with v_e , being largest close to critical rotation, and so small for the slowly rotating models ($v_e = 0.24v_c$) that they can barely be distinguished from their non-rotating neighbours.

The most striking aspect of Fig. 3 is the strong inclination (i) dependence of the trajectories in the $M_V/(B - V)$ plane. For the $i = 0^\circ$ models, rotation increases the observed brightness, owing to beaming of radiation from the hot pole; however, this increase happens without any appreciable variation in colour, leading to trajectories that are close to vertical. The converse occurs when $i = 90^\circ$: the centrifugal distention of equatorial regions produces a drop in the surface-averaged effective temperature,

reddening the colours at approximately constant brightness, and so resulting in nearly horizontal trajectories. For the intermediate, $i = 45^\circ$, case, a combination of brightening and reddening produces diagonal trajectories, coincidentally nearly parallel to those produced by the process of stellar evolution.

The increase in brightness for the pole-on models is approximately independent of subtype, being $\Delta M_V \approx -0.65$ mag at $v_e = 0.95v_c$, while the reddening of the equator-on models, at the same rotation rate, shows a modest increase from $\Delta(B - V) = 0.032$ mag at B0 to $\Delta(B - V) = 0.066$ mag at B9. By chance, the ratios between these brightening and reddening values correspond closely to the colour–magnitude slope of the main sequence throughout the B spectral type. Therefore, for an ensemble of randomly oriented B stars, the effect of gravity darkening owing to rotation at fixed values of v_e/v_c is to shift the main sequence up and to the right in the colour–magnitude diagram, but to leave it otherwise undistorted. We will return to this point in Section 6.3.

6 DISCUSSION

The calculations in Section 4 are intended to underline our central point that line widths are a rather poor indicator of $v_e \sin i$ at near-critical rotation. Although this basic idea has been previously noted in the literature (Stoeckley 1968; Hardorp & Strittmatter 1968b; Collins & Truax 1995), in practice it has been almost entirely ignored by observers (cf. Howarth 2002). For example, in the course of writing up this work we discovered that Stoeckley (1968, his fig. 4) gives a diagram that is very similar to our Fig. 1, while also addressing the implications for Be stars. However, the low citation rate for this paper (at the time of writing, a single citation⁵ in the ADS data base since 1975) suggests that the significance of this result for Be-star physics has been largely overlooked. In this section, therefore, we critically review the historical basis for the canonical view that v_e/v_c does not exceed ~ 0.8 for Be stars.

6.1 Line profiles

The basic method for determinations of $v \sin i$ is, of course, line-profile measurements. Slettebak’s (1982) observational study of rotation in a sample of 163 Be stars has been particularly influential; many authors have relied directly on his $v \sin i$ data (e.g. Porter 1996), or have used them to calibrate (e.g. Balona 1975; Halbedel 1996; Steele, Negueruela & Clark 1999; Yudin 2001; Abt, Levato & Grosso 2002) or to validate (e.g. Howarth et al. 1997; Chauville et al. 2001) their own measurements.

Slettebak (1982) used visual inspection of photographic spectra to estimate the line widths in his targets, calibrating his results with standards from Slettebak et al. (1975). This approach assumes a single-valued correspondence between line width and $v \sin i$, and neglects the redundancy between these parameters that we have emphasized. Slettebak is universally acknowledged as an exceptionally skilled observer, and we believe that his careful and conservative approach would have led him to adopt the *minimum* $v \sin i$ value consistent with his observations (rather than some arbitrarily

larger value), which, as we have shown, will generally underestimate $v_e \sin i$.

Furthermore, the $v \sin i$ values of the underpinning Slettebak et al. (1975) standard stars were themselves calibrated against theoretical profiles from Collins (1974). The latter’s pioneering calculations required computations that were, by the standards of the day, sophisticated and demanding. Unfortunately, subsequent results, including his own (cf. Collins & Truax 1995) and those we present here, shed some doubt on this fundamental calibration. For example, Collins (1974) found line broadening to be relatively unaffected by gravity darkening. Indeed, his paper explicitly notes a ‘remarkably good linear correlation between the theoretical value for $v_e \sin i$ and the half-width of the line’ – a correlation from which our gravity-darkened, complete models depart, quite significantly, in the crucial limit of large $v_e \sin i$ values (Fig. 1).

Collins’ remark was illustrated by calculations of the He I $\lambda 4471$ profile for a B0-type stellar model (his fig. 5). That figure indicates line half-widths at half depth that are systematically *broader* for critical rotators than for subcritical rotators at the same $v_e \sin i$ value. We find it difficult to devise any physical explanation for such behaviour, and suspect that it may indicate some procedural or coding error in his study. Indeed, later work by, e.g. Collins & Truax (1995) gives findings broadly consistent with our own, and also contradicts the linear correlation found by Collins (1974). In any event, our Table 2 indicates that the B0 subtype exhibits the smallest velocity deficiencies of any of the stellar models that we have considered. Therefore, notwithstanding any putative problems with Collins’ early calculations, we expect the data plotted in his fig. 5 to provide the poorest illustration of the degree to which gravity darkening can influence line broadening.

From the point of view of both observational procedure and underlying calibration, we are therefore led to the conjecture that the system of Be-star velocities underpinned by the work of Slettebak et al. (1975) and Slettebak (1982) may systematically underestimate $v_e \sin i$ values, particularly at the upper end of the rotation scale. This conjecture is given credence by the recent investigation by Chauville et al. (2001), who obtained $v \sin i$ values for 116 Be stars by least-squares fits of synthetic spectra to observed He I $\lambda 4471$ line profiles. As for our uniform models, the synthetic profiles of Chauville et al. (2001) were calculated under the assumption of no rotational distortion or gravity darkening, and they therefore certainly underestimate $v_e \sin i$. However, they obtained $v \sin i$ values in excellent overall agreement with those of Slettebak (1982), encouraging the view that there is also a systematic error in the latter’s results (and hence in all subsequent work built on them).

6.2 Statistics

Chauville et al. (2001) measured a mean projected equatorial velocity ($v \sin i/v_c$) = 0.65 for their sample of Be stars. Using the Chandrasekhar & Münch (1950) relationships between projected and intrinsic rotation velocities, they inferred from their data a mean equatorial velocity $\langle v_e/v_c \rangle = 0.83 \pm 0.03$. This extremely small apparent intrinsic scatter led them to conclude that ‘all studied Be stars rotate at nearly the same ratio [of] v_e/v_c ’.

We know of no physical reason why all Be stars should rotate at the same value of $v_e/v_c \simeq 0.8$, but examination of our Fig. 1 shows that at and above $v_e/v_c \simeq 0.8$ there is effectively no change in line width with increasing v_e . It is therefore reasonable to suppose that the observations may be consistent with *any* value (or a range of values) $\gtrsim 0.8$, and particularly with near-critical rotation – an obvious limiting value.

⁵ Collins & Truax (1995) cite Stoeckley’s work, and also give a similar diagram to our Fig. 1 (their fig. 4); but we disagree with their conclusion that an approximate treatment of limb darkening is the major factor in departures from the results of the uniform model. Note that even our simple, uniform models incorporate a detailed treatment of non-linear, wavelength-dependent limb darkening.

To investigate this possibility in a heuristic way, we consider a population of complete B2-star models with equatorial velocities distributed uniformly between $v_e = 0.93v_c$ and $v_e = 0.97v_c$, and with rotation axes oriented randomly. Analysing this population with He I $\lambda 4471$ line profiles derived from our uniform models (thereby effectively mimicking the procedure of Chauville et al. (2001)), we obtain a mean projected equatorial velocity of $\langle v \sin i / v_c \rangle = 0.635$, from which the Chandrasekhar & Münch (1950) relationships suggest a mean equatorial velocity $\langle v_e / v_c \rangle = 0.809$, with a variance $\sigma^2(v_e / v_c) = -9 \times 10^{-3}$. These *inferred* values⁶ are remarkably close to those obtained by Chauville et al., even though our synthetic population rotates at significantly more rapid rates than the $\langle v_e / v_c \rangle = 0.83$ advanced by those authors. Of course, this simulation is not particularly realistic, but it none the less clearly establishes that statistical studies that do not adequately treat the effects of gravity darkening must inevitably lead to systematic underestimates of $v_e \sin i$.

6.3 Photometry

The calculations in Section 5 indicate that near-critical rotation (by which we mean $v_e / v_c \simeq 0.95$) displaces stars toward brighter magnitudes or redder colours, depending on the inclination. This phenomenon, first discovered by Roxburgh & Strittmatter (1965), has been investigated and confirmed by a number of authors (e.g. Collins 1966; Faulkner, Roxburgh & Strittmatter 1968; Hardorp & Strittmatter 1968a; Maeder & Peytremann 1970). Our qualitative findings are very similar to these studies, although we obtain smaller changes in brightness ($\Delta M_V \simeq -0.6$ mag) and colour ($\Delta(B - V) \simeq 0.06$ mag) than found historically (for reasons we discuss below).

Evidently, if Be stars are indeed near-critical rotators, they should naturally occupy a brighter/redder position in the colour–magnitude diagram than normal B-type stars. A search through the relevant literature reveals substantive evidence for such an anomalous position: Zorec & Briot (1991) find their sample of Be stars to be overluminous with respect to main-sequence stars, and of the 14 previous studies that they cite, 11 disclose similar behaviour.

In the era when the observational consequences of gravity darkening were first being investigated, it was natural to attribute this observed overluminosity to rapid rotation (e.g. Stoeckley 1968). However, many of the studies from the 1960s (including the majority of those we cite above) were based on stellar interior calculations by Roxburgh, Griffith & Sweet (1965), which were found by Sander-son, Smith & Hazlehursts (1970) to contain a serious error. Correction of this error resulted in a reduction of the brightness/reddening change caused by rotation (towards values commensurate with those we found in Section 5), to such an extent that rotation alone was hard-pushed to explain the luminosity anomaly.

Ever since the error by Roxburgh et al. (1965) was discovered there has been a shift towards interpreting the anomaly as a consequence of the circumstellar emission (CE) produced by the discs of Be stars (e.g. Fabregat et al. 1996). This hypothesis certainly seems promising, but it has never been established whether CE can explain the observations *in toto*; as Zorec & Briot (1997) point out, it may be the case that multiple mechanisms (including rapid rotation) are

⁶ Note that the variance for our synthetic population is less than zero owing to the marginal breakdown of the assumption by Chandrasekhar & Münch (1950) that the $v \sin i$ distribution arises from the spatial projection of an intrinsic distribution.

required to explain the anomalous position of Be stars in the colour–magnitude diagram. Indeed, it is still not clear what the effects are of the intrinsic ‘rotation reddening’ discussed by Maeder (1975), which arise from the distention of the envelope around the equatorial regions of a rapidly rotating star (such that the local atmospheric structure departs from that predicted by plane-parallel models).

6.4 Future approaches

Having presented evidence that current measurements of Be-star rotation are underestimates, let us briefly consider what approaches might be deployed in the future to address this problem. To reiterate, the essence of the problem is this: when a star rotates at a significant fraction of its critical velocity v_c , the insensitivity of line widths toward any further increase in the rotation rate means that these widths are poor indicators of the true projected equatorial velocity of the star $v_e \sin i$. How might this degeneracy be lifted?

One possible approach lies in leveraging the combined temperature/wavelength dependence of the continuum flux. From far-ultraviolet (FUV) observations of Be stars, Heap (1976) discovered the line broadening at these wavelengths to be significantly less than at visible wavelengths. As pointed out by Hutchings (1976), this effect can be understood as a result of the different surface brightness distributions at visible and FUV wavelengths, caused by gravity darkening. Hutchings & Stoeckley (1977) subsequently suggested that the effect might be used to obtain reliable values for v_e / v_c and i . Such an approach certainly looks promising, but suffers from the drawback of requiring simultaneous visible, FUV and (if possible) infrared observations, which are often difficult to secure.

An alternative technique for lifting the degeneracy lies in exploiting the differing temperature sensitivities of different spectral lines. As we demonstrated in Sections 4.2–4.3, the inverse temperature/EW dependence exhibited by the Mg II $\lambda 4481$ line partly counteracts the effect of gravity darkening in the continuum, and lessens the impact of the degeneracy. In the case of an individual line such as this, the effect will probably be too small to be of practical use,⁷ but the effect could be exploited by simultaneous modelling of *multiple* lines. In principle, the different temperature/EW dependence of each line means that a good fit for *all* lines will occur only at a single point in parameter space (i.e. a single combination of v_e , i , M_* etc.). In reality, of course, noise and other factors will limit the precision of this approach; nevertheless, the approach certainly appears promising, and has already been applied with success to rapidly rotating O stars (see Howarth & Smith 2001).

The most direct method for examining rotational distortion is through imaging. Once the aspect ratio $x \equiv R_e / R_p$ of the centrifugally distorted star is known, its equatorial velocity can be calculated in the Roche approximation from

$$\frac{v_e}{v_c} = x \sqrt{\frac{3(x-1)}{x^3}}, \quad (4)$$

where we note that $x = 1.5$ corresponds to $v_e / v_c = 1$. Recently, Domiciano de Souza et al. (2003) applied this approach to the Be star α Eri; their *VLTI* observations indicate an aspect ratio entirely consistent with near-critical rotation. Clearly, the power of this approach lies in its ability to avoid the need for complex modelling

⁷ We also note on more general grounds that the Mg II $\lambda 4481$ line is a suboptimal choice for $v_e \sin i$ determination, owing to blending with the adjacent He I $\lambda 4471$ line for rapid rotators.

of stellar atmospheres or interiors. Unfortunately, its applicability is limited to those stars which are resolvable via interferometry.

7 CONCLUSION

We have argued that the available observations, and their interpretation, leave open the possibility that Be stars rotate at or near to their critical velocities, contrary to the previous consensus. In questioning the canonical view that Be-star rotation is substantially sub-critical, we have been motivated by the issue of the fundamental physical processes responsible for the Be phenomenon. A range of phenomenological models have been developed to account for various aspects of Be-star behaviour, some quite detailed and sophisticated (e.g. Okazaki 1991), but the mechanisms underlying the formation of circumstellar discs remain elusive. This is largely owing to the substantial energetic requirements for levitating material in a strong gravitational field.

Near-critical rotation alleviates this problem to the point where known processes, such as pulsation or gas pressure, may readily provide sufficient energy and angular momentum. Our critique argues that such near-critical rotation *has not* been ruled out by existing studies, be they spectroscopic or photometric. Indeed, these studies furnish *necessary* evidence that the Be stars *are* rotating close to critical; we hope that this paper will provide motivation towards obtaining *sufficient* evidence in support of the same conclusion, perhaps using one of the approaches we suggest in Section 6.4.

ACKNOWLEDGMENTS

We thank Dietrich Baade and Thomas Rivinius for their helpful suggestions toward improving the paper, and Antonio Claret for the generous provisions of his flux data. RHDT acknowledges PPARC support. SPO received support from a PPARC fellowship for sabbatical research in the UK, and from NSF grant no. AST00-97983 to the University of Delaware. IDH is a Jolligoode fellow.

REFERENCES

- Abt H. A., Levato H., Grosso M., 2002, *ApJ*, 573, 359
 Allen C. W., 1976, *Astrophysical Quantities*, 3rd edn. Athlone, London
 Balona L. A., 1975, *MemRAS*, 78, 51
 Carroll J. A., 1928, *MNRAS*, 88, 548
 Chandrasekhar S., Münch G., 1950, *ApJ*, 111, 142
 Chauville J., Zorec J., Ballereau D., Morrell N., Cidale L., Garcia A., 2001, *A&A*, 378, 861
 Claret A., 2000, *A&A*, 363, 1081
 Collins G. W., 1966, *ApJ*, 146, 914
 Collins G. W., 1974, *ApJ*, 191, 157
 Collins G. W., Truax R. J., 1995, *ApJ*, 439, 860
 Cranmer S. R., 1996, PhD thesis, Univ. Delaware
 Dachs J., Hanuschik R., Kaiser D., Rohe D., 1986, *A&A*, 159, 276
 Domiciano de Souza A., Kervella P., Jankov S., Abe L., Vakili F., di Folco E., Paresce F., 2003, *A&A*, 407, L47
 Dziembowski W. A., Pamyatnykh A. A., 1993, *MNRAS*, 262, 204
 Dziembowski W. A., Moskalik P., Pamyatnykh A. A., 1993, *MNRAS*, 265, 588
 Fabregat J., Torreyon J. M., Reig P., Bernabeu G., Busquets J., Marco A., Reglero V., 1996, *A&AS*, 119, 271
 Faulkner J., Roxburgh I. W., Strittmatter P. A., 1968, *ApJ*, 151, 203
 Gray D. F., 1992, *The Observation and Analysis of Stellar Photospheres*. Cambridge Univ. Press, Cambridge
 Halbedel E. M., 1996, *PASP*, 108, 833
 Hanuschik R. W., 1996, *A&A*, 308, 170
 Hardorp J., Strittmatter P. A., 1968a, *ApJ*, 151, 1057
 Hardorp J., Strittmatter P. A., 1968b, *ApJ*, 153, 465
 Heap S. R., 1976, in Slettebak A., ed., *Proc. IAU Symp. 70, Be and Shell Stars*. Reidel, Dordrecht, p. 165
 Howarth I. D., 2002, in Maeder A., Eenens P., eds, *Proc. IAU Symp. 215, Stellar Rotation*. Astron. Soc. Pac., San Francisco, in press
 Howarth I. D., Smith K. C., 2001, *MNRAS*, 327, 353
 Howarth I. D., Siebert K. W., Hussain G. A. J., Prinja R. K., 1997, *MNRAS*, 284, 265
 Hubeny I., 1988, *Comp. Phys. Commun.*, 52, 103
 Hubeny I., Lanz T., 1995, *ApJ*, 439, 875
 Hutchings J. B., 1976, *PASP*, 88, 5
 Hutchings J. B., Stoeckley T. R., 1977, *PASP*, 89, 19
 Iglesias C. A., Rogers F. J., 1996, *ApJ*, 464, 943
 Kurucz R., 1993, CD-ROM No. 16. Smithsonian Astrophysical Observatory, Washington DC
 Maeder A., 1975, *A&A*, 42, 471
 Maeder A., Meynet G., 2000, *ARA&A*, 38, 143
 Maeder A., Peytremann E., 1970, *A&A*, 7, 120
 Morgan W. W., Keenan P. C., 1973, *ARA&A*, 11, 29
 Okazaki A. T., 1991, *PASJ*, 43, 75
 Owocki S. P., 2002, in Maeder A., Eenens P., eds, *Proc. IAU Symp. 215, Stellar Rotation*. Astron. Soc. Pac., San Francisco, in press
 Porter J. M., 1996, *MNRAS*, 280, L31
 Rogers F. J., Swenson F. J., Iglesias C. A., 1996, *ApJ*, 456, 902
 Roxburgh I. W., Strittmatter P. A., 1965, *Z. Astrophys.*, 63, 15
 Roxburgh I. W., Griffith J. S., Sweet P. A., 1965, *Z. Astrophys.*, 61, 203
 Sanderson A. D., Smith R. C., Hazlehurst J., 1970, *ApJ*, 159, L69
 Secchi A., 1867, *Astron. Nachr.*, 68, 63
 Shajn G., Struve O., 1929, *MNRAS*, 89, 222
 Slettebak A., 1949, *ApJ*, 110, 498
 Slettebak A., 1966, *ApJ*, 145, 126
 Slettebak A., 1982, *ApJS*, 50, 55
 Slettebak A., Collins G. W., Parkinson T. D., Boyce P. B., White N. M., 1975, *ApJS*, 29, 137
 Slettebak A., Kuzma T. J., Collins G. W., 1980, *ApJ*, 242, 171
 Slettebak A., Collins G. W., Truax R., 1992, *ApJS*, 81, 335
 Smith M. A., Gray D. F., 1976, *PASP*, 88, 809
 Smith M. A., Henrichs H. F., Fabregat J., 2000, eds, *ASP Conf. Ser. 214, Proc. IAU Colloq. 175, The Be Phenomenon in Early-Type Stars*. Astron. Soc. Pac., San Francisco
 Steele I. A., Negueruela I., Clark J. S., 1999, *A&AS*, 137, 147
 Stoeckley T. R., 1968, *MNRAS*, 140, 141
 Struve O., 1931, *ApJ*, 73, 94
 Townsend R. H. D., 1997, *MNRAS*, 284, 839
 von Zeipel H., 1924, *MNRAS*, 84, 665
 Yudin R. V., 2001, *A&A*, 368, 912
 Zorec J., Briot D., 1991, *A&A*, 245, 150
 Zorec J., Briot D., 1997, *A&A*, 318, 443

This paper has been typeset from a $\text{\TeX}/\text{\LaTeX}$ file prepared by the author.